Supplement of Earth Surf. Dynam., 9, 295–315, 2021
https://doi.org/10.5194/esurf-9-295-2021-supplement

Earth Surface Dynamics
Open Access

Supplement of

Development of smart boulders to monitor mass movements via the Internet of Things: a pilot study in Nepal

Benedetta Dini et al.

Correspondence to: Benedetta Dini (b.dini@uea.ac.uk)

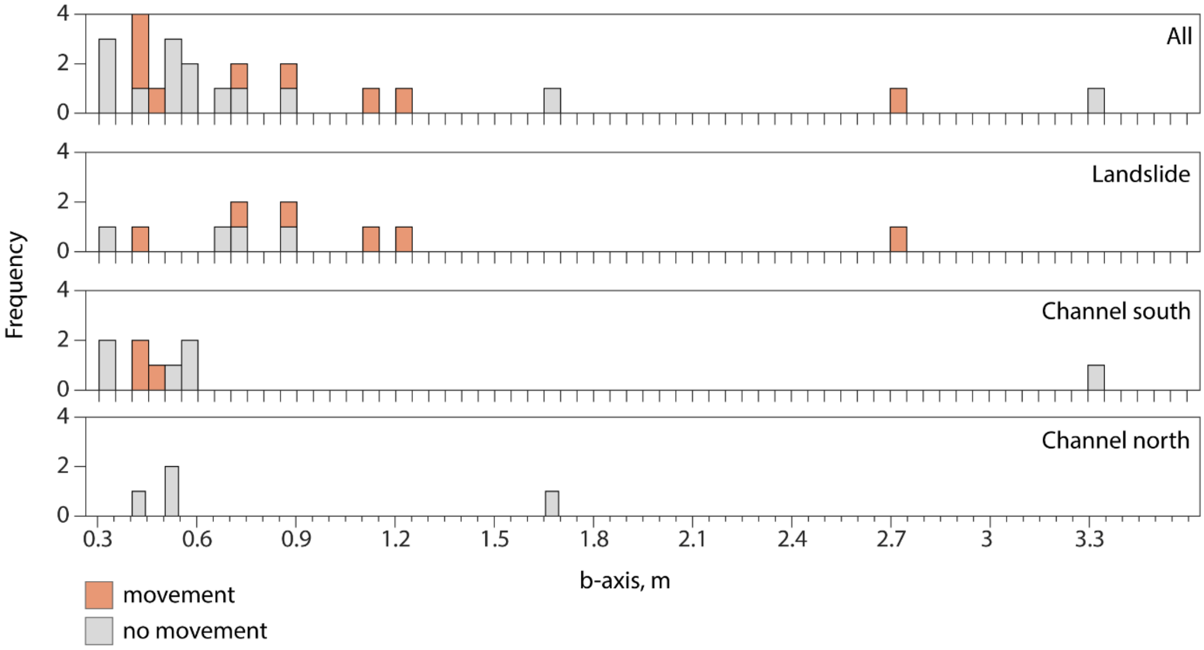

Fig. S1. Histograms of boulders b-axis. Colours indicate boulders with movement (light red) or no movement (grey), whilst the panels, top to bottom represent all boulders, landslide boulders, and boulders in the south and north channels respectively. Boulders within the landslide show movements even when their sizes are large, whilst those in the southern channel had preferentially b-axis between 0.4 and 0.5 m.

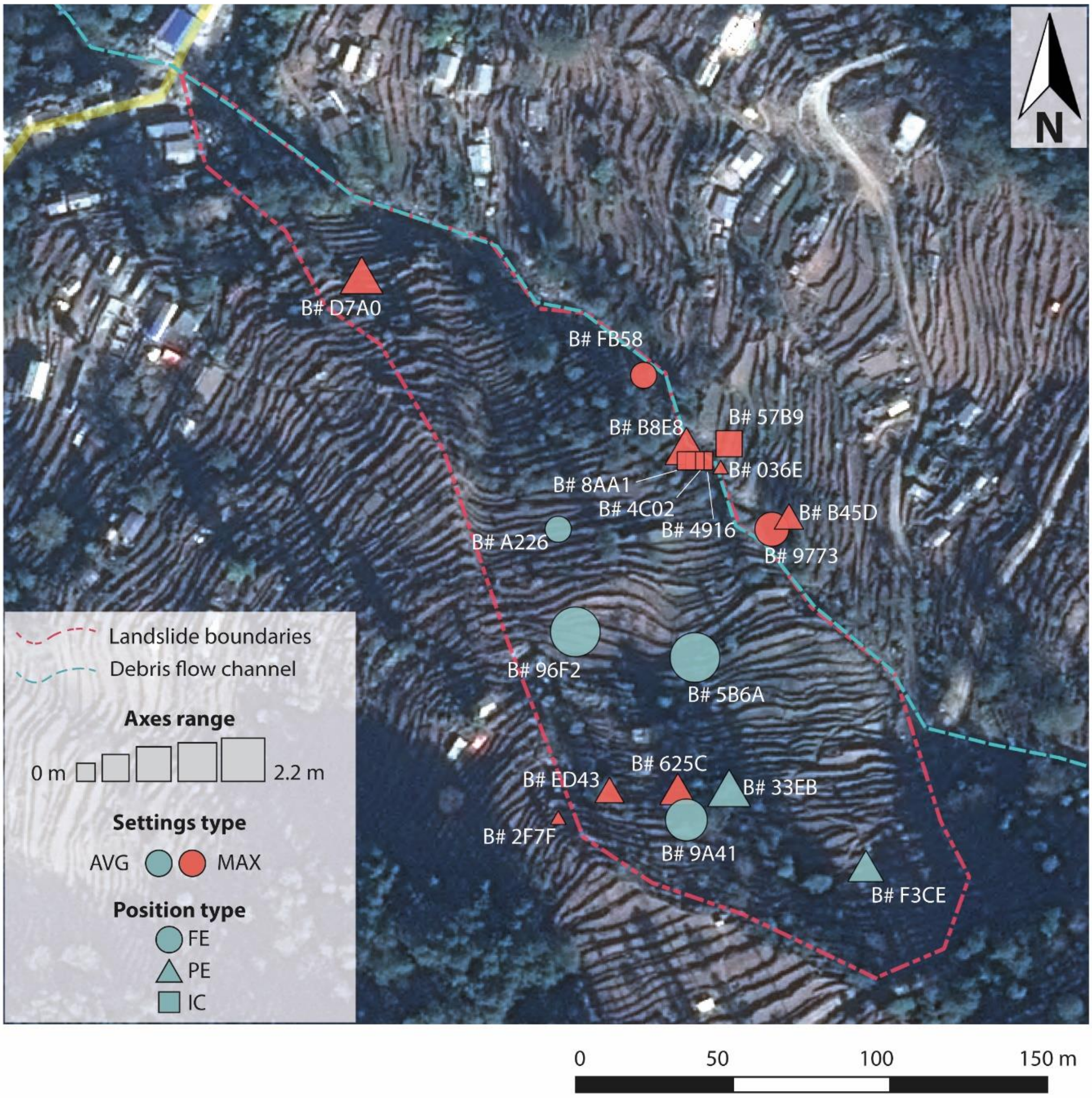

Fig. S2. Zoom of two tagged sites. Sizes represent the range between the a-axis and the c-axis of the boulders (equal axes, range 0; most elongated boulders, range 2.2). Sizes are shown in legend for squared symbols but apply to all boulders. Colours represent setting types and symbols represent location type. Image: Pleiades (CEOS Landslides Pilot).

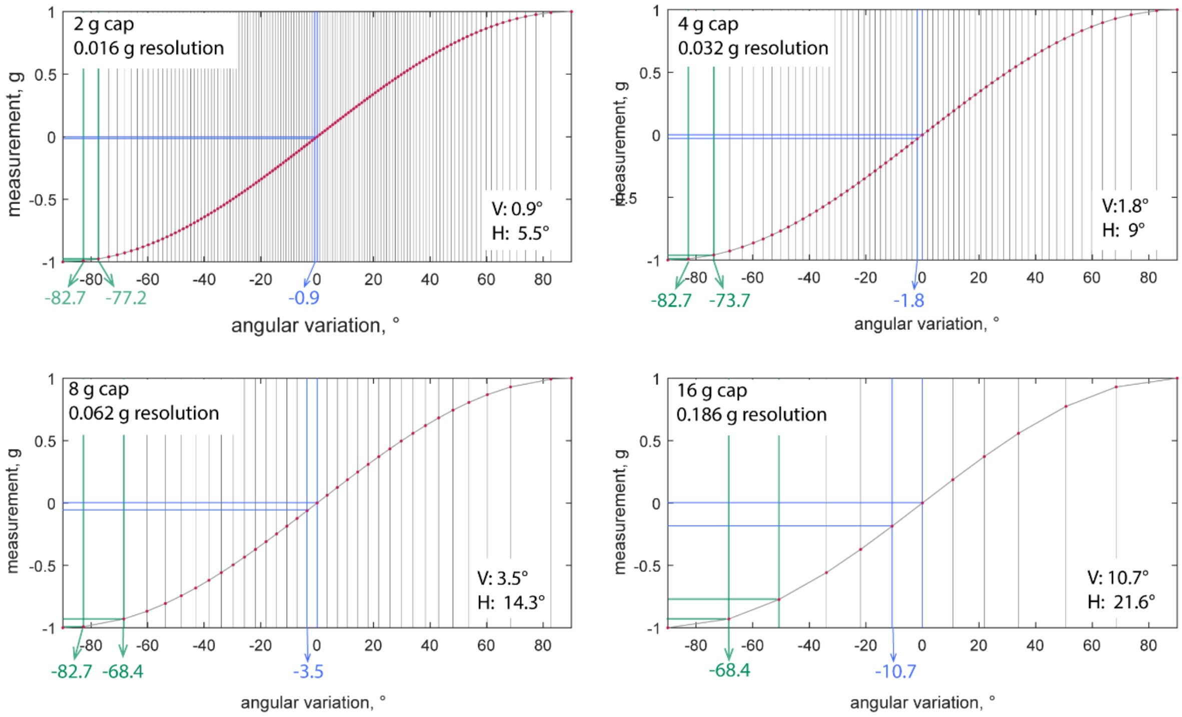

Fig. S3. Resolution and sensitivity of the accelerometer with scale capped at 2, 4, 8, and 16 g respectively. The vertical lines represent the angular variation corresponding to each step in the scale (mg). The graphs show that for increasing maximum detectable value, the resolution decreases significantly. Moreover, the sensitivity is higher when the axis is vertical than when the axis is horizontal, i.e. when the axis is near horizontal, a larger angular variation is required to make one step in the g scale. Thus, the angular threshold used to trigger a fix has to be higher than the maximum angular change needed to make a step in the g scale when the axis is near horizontal. This is shown as H in the text box in the plots.

Supplement section S1

For the visualisations shown in figure 6B, D and F we used the following equations, in order to calculate the change in orientation that must have occurred between **two successive static measurements**:

$$\vartheta = \tan^{-1} \frac{Acc_x}{\sqrt[2]{{Acc_y}^2 + {Acc_z}^2}} \tag{1}$$

$$\varphi = \tan^{-1} \frac{Acc_y}{\sqrt[2]{{Acc_x}^2 + {Acc_z}^2}} \tag{2}$$

where ϑ and φ are the pitch and roll angles in a Euler system respectively.

As the yaw angle cannot be calculated with accelerometer data alone, the visualisations proposed in figure 6B, D and F show model boulders in a space with no coordinates. This is because these boulders do not represent the real boulders placed in the real slope system. The aim of these visualisations is only to give the sense to the reader of the minimum change required in the orientation of the boulders to give the observed change in static tilt in x, y, z. As we explain in the main text, the delay induced by the GPS acquisition and the accelerometer sampling frequency would not allow for a full 3D representation of the whole movement as it unfolded.

Essentially, the equations above were used to show the orientation change in pitch and roll angles that occurred at different stages of our time series. The different stages are indicated in figures 6A, C and D as numbers, corresponding to jumps in the x, y, z values in the time series. The new acquired orientation in terms of pitch and roll angles is shown for each corresponding stage in figures 6B, D and F.